Front. Mech. Eng. 2021, 16(1): 176–185
https://doi.org/10.1007/s11465-020-0616-0

RESEARCH ARTICLE

Qun CHAO, Jianfeng TAO, Junbo LEI, Xiaoliang WEI, Chengliang LIU, Yuanhang WANG, Linghui MENG

Fast scaling approach based on cavitation conditions to estimate the speed limitation for axial piston pump design

Abstract The power density of axial piston pumps can benefit greatly from increased rotational speeds. However, the maximum rotational speed of axial piston machines is limited by the cavitation phenomenon for a given volumetric displacement. This paper presents a scaling law derived from an analytical cavitation model to estimate the speed limitations for the same series of axial piston pumps. The cavitation model is experimentally verified using a high-speed axial piston pump, and the scaling law is validated with open specification data in product brochures. Results show that the speed limitation is approximately proportional to the square root of the inlet pressure and inversely proportional to the cube root of volumetric displacement. Furthermore, a characteristic constant C_p is defined based on the presented scaling law. This constant can represent the comprehensive capacity of axial piston pumps free from cavitation.

Keywords axial piston pump, cavitation, speed limitation, scaling law

1 Introduction

Axial piston pumps are essential elements in fluid power transmission systems; they supply pressurized fluid to actuator components by converting rotational mechanical power into hydraulic fluid power. These pumps have various applications in construction, agriculture, mining, aerospace, and robotics because of their high power density, high efficiency, available displacement control, and long service life. Power density has become a crucial attribute of axial piston pumps, especially in mobile and aerospace applications, because it can help meet increasingly strict requirements on weight and installation space. It is defined as the ratio of output power to mass [1]. This definition indicates that the power density of axial piston pumps can be improved by two approaches. The first approach is to increase the output power by increasing the discharge pressure, but the maximum pressure is predetermined by the hydraulic system and material strength [2,3]. The second approach is to decrease the pump mass by improving the rotational speed because for a certain delivery flow rate, an axial piston pump with a high speed capacity can be designed with a small volumetric displacement [4]. For example, pump mass can be greatly reduced by five times when the maximum rotational speed of aircraft hydraulic pumps is increased from 4000 to 15000 r/min. In recent years, the use of high-speed axial piston pumps in integrated electro-hydrostatic actuators where the electric motor directly drives a small-displacement axial piston pump has become popular [5,6].

Although the power density of axial piston pumps benefits considerably from high rotational speeds, the maximum speed of axial piston pumps is limited by several mechanical restrictions, such as slipper tipping [7–9], cylinder block tipping [10–12], and load–velocity relationships (PV factors) of friction pairs [13]. Cavitation is another common factor that limits the speed of axial piston pumps. Kunkis and Weber [3] claimed that cavitation usually occurs far before the above mentioned mechanical limits; thus, the terminus speed limitation of axial piston pumps is determined largely by cavitation.

Many researchers have investigated the cavitation in axial piston pumps experimentally and numerically. They found that the combination of high rotational speed and insufficient suction poses a high risk of cavitation in axial piston pumps [14–17] and consequently leads to various problems, such as low volumetric efficiency [18,19],

Received August 2, 2020; accepted September 29, 2020

Qun CHAO, Jianfeng TAO, Junbo LEI (✉), Xiaoliang WEI, Chengliang LIU
State Key Laboratory of Mechanical System and Vibration, School of Mechanical Engineering, Shanghai Jiao Tong University, Shanghai 200240, China
E-mail: jblei@sjtu.edu.cn

Yuanhang WANG, Linghui MENG
China Electronic Product Reliability and Environmental Testing Research Institute, Guangzhou 510610, China

vibration and noise [19,20], and erosion damage [21,22]. Furthermore, pump cavitation has adverse effects on the entire hydraulic system. For example, the flow rate and bulk modulus of the pumping fluid are reduced by cavitation, and this reduction results in a slow dynamic response of the hydraulic system [23].

Several common methods are utilized to prevent the cavitation of axial piston pumps in engineering practice. The first method is to boost the inlet pressure by pressurizing the tank [24] or adding an integral boost impeller [25] at the end of the shaft. Cavitation suppression can be also achieved by minimizing the pressure loss from the inlet port to the cylinder chamber [26]. Typical optimization designs for flow passage include special-shaped suction lines [27,28], spherical valve plates [29], and inclined cylinder ports [3,15]. Another common method for realizing low cavitation in axial piston pumps is to reduce the reverse flow between the cylinder chamber and the pump port by carefully designing the valve plate [30,31].

Previous studies have shown that cavitation is an important issue to be considered in axial piston pump design, and most of them have focused on cavitation simulations and experiments and optimization designs of components. Their results provide useful guidelines for preventing cavitation in axial piston pumps. Pump manufacturers face a growing demand for the development of new machines on the basis of the successful design of the same product family. Particularly, pump engineers are greatly concerned about how to consider the cavitation factor when estimating the speed limitations of a new scaled machine at its preliminary design phase [32].

This study aims to explore a fast scaling approach for estimating the speed limitation of axial piston pumps on the basis of cavitation restriction. First, an analytical model for cylinder cavitation is developed and experimentally verified by using a high-speed axial piston pump. Second, a fast scaling law for estimating the speed limitation of axial piston pumps is derived from the analytical model of cavitation. Lastly, the speed limitation data of a family of axial piston pumps are collected from product brochures to confirm the validity of the scaling method.

2 Machine description

Figure 1 schematically shows the general configuration of a swash-plate-type axial piston pump, in which only the main characteristics of the pump are presented; several design details are not considered because of their lack of generality. The axial piston pump completes its suction and discharge strokes by changing the displacement chamber volume periodically. The cylinder block accommodates an odd number of pistons (e.g., 7, 9, or 11) at equal angular intervals about its centerline. Each piston is connected to a slipper via a ball joint, which allows the slipper to rotate around the piston ball. The slippers are held against an angled swash plate by using a hold-down device (not shown in Fig. 1), and the cylinder block is pushed toward the stationary valve plate by a compressed spring nested in the cylinder cavity. The shaft is coupled with the cylinder block by a spline mechanism, and the rotating group (including the shaft, cylinder block, pistons, and slippers) is supported by two bearings at the shaft ends.

Once the shaft drives the cylinder block to rotate, the slippers slide against the swash plate and force the pistons to reciprocate within the cylinder bores. As a result, displacement chambers are formed between the cylinder block and pistons and varied periodically. The low-pressure hydraulic fluid flows into the displacement chambers from the valve plate opening as the pistons are drawn out of the cylinder block in the suction stroke. By contrast, the high-pressure hydraulic fluid flows out of the other valve plate opening as the pistons are pushed into the cylinder block in the discharge stroke. These suction and discharge strokes are repeated for each revolution of the cylinder block to accomplish the basic task of delivering hydraulic fluid continuously.

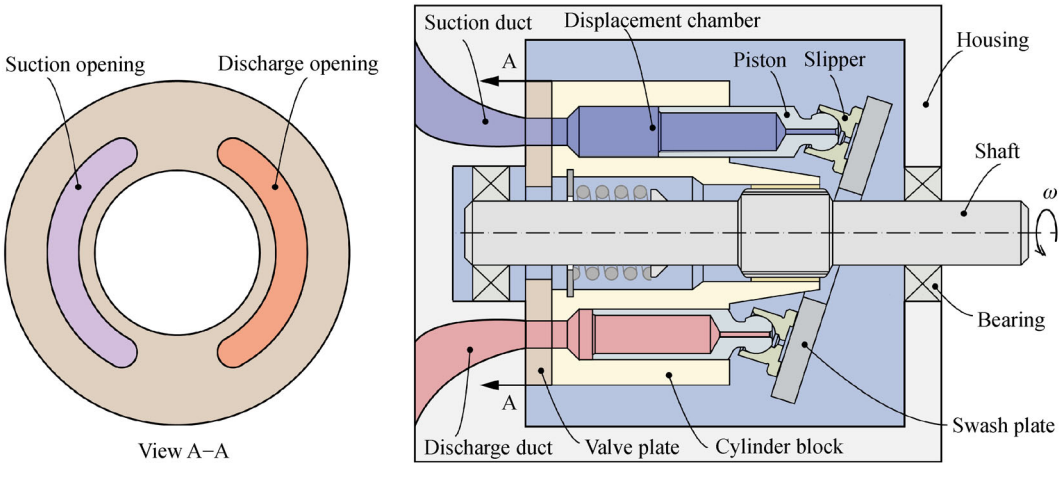

Fig. 1 Schematic of a swash-plate-type axial piston pump.

3 Analytical model for cavitation in displacement chambers

The results of Refs. [3,14,15] suggest that axial piston machines are likely to suffer from cavitation in the displacement chambers during suction stroke. Therefore, this study focuses on the cavitation in the displacement chambers at the suction side. Cavitation can be generated in the displacement chambers when the fluid pressure drops below the air saturation or vaporization pressure. Generally, the air saturation pressure is much higher than the vaporization pressure for the hydraulic fluid; thus, gaseous cavitation occurs before vaporous cavitation [17].

The hydraulic fluid gradually consumes its pressure when it travels from the stationary pump inlet to the movable displacement chambers, where the following factors contribute to the total pressure drop [33,34]. First, the inlet pressure is consumed partially as the supplied fluid flows from the pump inlet to the cylinder ports due to the friction loss in the inlet line and flow expansion. Second, the fluid pressure continues to drop as the entering fluid accelerates to the cylinder block's rotational speed and the piston's linear velocity to fill the increased void volume of the displacement chambers. Aside from these two types of pressure loss, the centrifugal effects of the rotating fluid also cause a local pressure drop in the displacement chambers [14,15,35]. The first portion of the pressure loss varies considerably from one pump to another; therefore, it is not considered in this work for mathematical simplicity.

The cavitation analysis of axial piston pumps begins with computing the fluid pressure in the cylinder chambers. Figure 2 schematically illustrates a cylinder chamber filled with the entering hydraulic fluid. The following assumptions are established for the derivation of the displacement chamber pressure:

1) The viscous and gravity forces of the entering fluid are negligibly small compared with the inertial forces;

2) The entering fluid is incompressible, and the fluid flow is steady.

Three coordinates are defined in Fig. 2 to describe the movement of the entering fluid in the cylinder chambers. The global coordinate system (X, Y, Z) has its origin at the intersection of the cylinder block's centerline and bottom surface. The Z-axis coincides with the cylinder block's centerline, and its positive direction goes from the valve plate side to the swash plate side. The positive Z-axis is directed upward, and the X-axis is determined based on the right-hand rule. An equivalent cylindrical coordinate system (r, φ, Z) is introduced to describe the movement of the cylinder fluid in cylindrical coordinates, and it has the same origin and Z-axis as the (X, Y, Z) system. The coordinate φ is measured from the Y-axis, and its positive direction is assumed to be counterclockwise rotation. In addition, a local coordinate system (x_c, y_c, z_c) is defined using a reference cylinder bore. The origin of the (x_c, y_c, z_c) system is located at the bore centerline. The positive x_c-axis is always tangential to the piston pitch circle, and the positive y_c-axis is directed radially outward. Similarly, an equivalent cylindrical coordinate (r_c, θ, z_c) is defined based on the coordinate system (x_c, y_c, z_c), and each of its axes is shown in Fig. 2.

Consider an entering fluid particle P moving from the valve plate opening to the cylinder chamber. The fluid flow is governed by Navier–Stokes (N–S) equations, which describe the relationship between pressure and velocity. However, very few analytical solutions to these basic differential equations can be obtained for practical fluid flow problems. Therefore, in this work, we determine their approximate analytical solutions on the basis of several assumptions. When the viscous forces are disregarded, the complicated N–S equations are reduced to simple Euler's equations, which can be compactly expressed in vector notation as

$$\rho\frac{\mathrm{D}\boldsymbol{V}}{\mathrm{D}t}=\rho\boldsymbol{f}-\nabla p, \tag{1}$$

where ρ denotes fluid density, $\boldsymbol{V}$ denotes the velocity vector of the fluid particle, $\boldsymbol{f}$ denotes the body force vector, and p denotes cylinder chamber pressure.

For a steady flow, the total derivative $\mathrm{D}\boldsymbol{V}/\mathrm{D}t$ can be expressed as

$$\frac{\mathrm{D}\boldsymbol{V}}{\mathrm{D}t}=\nabla\left(\frac{1}{2}V^2\right)+(\nabla\times\boldsymbol{V})\times\boldsymbol{V}. \tag{2}$$

Substituting Eq. (2) into Eq. (1) produces the following

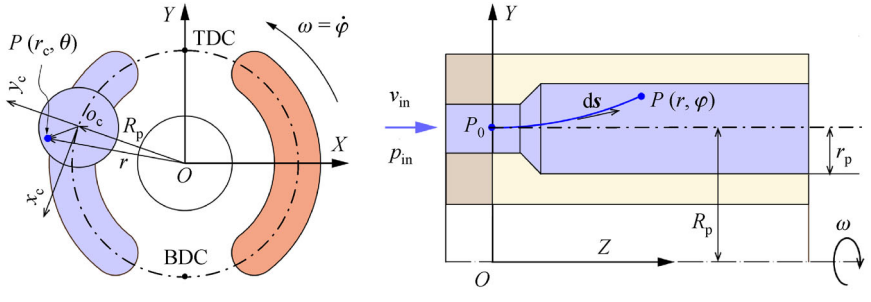

Fig. 2 Schematic of the fluid-filled cylinder chamber.

alternate expression of the Euler's equations:

$$\nabla\left(\frac{1}{2}V^2\right)+(\nabla\times\boldsymbol{V})\times\boldsymbol{V}=\boldsymbol{f}-\frac{1}{\rho}\nabla p. \tag{3}$$

To describe the rotating fluid, the Euler's equations are expressed in terms of the cylindrical coordinate system (r, φ, Z) as follows:

$$\nabla\left(\frac{1}{2}V_{\mathrm{r}}^2\right)+(\nabla\times\boldsymbol{V}_{\mathbf{r}})\times\boldsymbol{V}_{\mathbf{r}} =-\boldsymbol{\omega}\times(\boldsymbol{\omega}\times\boldsymbol{r})-\dot{\boldsymbol{\omega}}\times\boldsymbol{r}-2\boldsymbol{\omega}\times\boldsymbol{V}_{\mathbf{r}}-\frac{1}{\rho}\nabla p, \tag{4}$$

where $\boldsymbol{V}_{\mathrm{r}}$ and $\boldsymbol{r}$ are the relative velocity and position vectors of the fluid particle with respect to the rotating cylinder block, respectively, and $\boldsymbol{\omega}$ is the angular velocity vector of the cylinder block.

In the case of constant angular velocity and parallel cylinder bores, the second and third terms on the right side of Eq. (4) become zero. Thus, Eq. (4) is simply reduced to

$$\nabla\left(\frac{1}{2}V_{\mathrm{r}}^2\right)+(\nabla\times\boldsymbol{V}_{\mathbf{r}})\times\boldsymbol{V}_{\mathbf{r}} =-\boldsymbol{\omega}\times(\boldsymbol{\omega}\times\boldsymbol{r})-\frac{1}{\rho}\nabla p=\nabla\left(\frac{1}{2}\omega^2r^2\right)-\frac{1}{\rho}\nabla p. \tag{5}$$

Taking dot product of each term in Eq. (5) with a differential length d$\boldsymbol{s}$ along the streamline and integrating it result in

$$\frac{1}{2}V_{\mathrm{r}}^2-\frac{1}{2}\omega^2r^2+\frac{1}{\rho}p=C, \tag{6}$$

where the integration constant C can be determined from the velocity and pressure boundary conditions, V_{r} ($r=R_{\mathrm{p}}$) = v_{in} and p ($r=R_{\mathrm{p}}$) = p_{in}, where p_{in} and v_{in} are the static pressure and entering velocity of particle P at the valve plate opening, respectively, and R_{p} is the piston pitch radius.

The fluid pressure at an arbitrary location can be derived from Eq. (6) as follows:

$$p=p_{\mathrm{in}}+\frac{1}{2}\rho v_{\mathrm{in}}^2-\frac{1}{2}\rho V_{\mathrm{r}}^2+\frac{1}{2}\rho\omega^2(r^2-R_{\mathrm{p}}^2). \tag{7}$$

If the flow resistance between the pump inlet and valve plate opening is disregarded, the sum of the first two terms on the right side of Eq. (7) can be substituted by inlet pressure P_{in} according to the Bernoulli equation. In addition, the relative velocity V_{r} of the fluid flow with respect to the rotating cylinder block is expressed as

$$V_{\mathrm{r}}=\omega R_{\mathrm{p}}\tan\alpha\sin\varphi, \tag{8}$$

where α is the swash-plate angle, and φ is the angular displacement of the cylinder block.

Substituting Eq. (8) into Eq. (7) yields the final expression for static fluid pressure in the displacement chambers during the suction phase.

$$p=P_{\mathrm{in}}-\frac{1}{2}\rho\omega^2(R_{\mathrm{p}}^2\tan^2\alpha\sin^2\varphi-r^2+R_{\mathrm{p}}^2),$$

$$0^\circ\leqslant\varphi\leqslant360^\circ \text{ and } R_{\mathrm{p}}-r_{\mathrm{p}}\leqslant r\leqslant R_{\mathrm{p}}+r_{\mathrm{p}}, \tag{9}$$

where r_{p} is the piston radius.

The fluid pressure must be higher than air saturation pressure p_{a} to prevent gaseous cavitation in the displacement chambers. Equation (9) indicates that for a given axial piston machine, fluid pressure p is determined by inlet pressure and rotational speed. The required inlet pressure for avoiding cavitation is

$$P_{\mathrm{in}}\geqslant p_{\mathrm{a}}+\frac{1}{2}\rho\omega^2R_{\mathrm{p}}^2(\tan^2\alpha+2\lambda-\lambda^2), \tag{10}$$

where $\lambda=r_{\mathrm{p}}/R_{\mathrm{p}}$.

Similarly, the acceptable rotational speed for avoiding cavitation can be derived from Eq. (9) as follows:

$$\omega\leqslant\sqrt{\frac{2(P_{\mathrm{in}}-p_{\mathrm{a}})}{\rho R_{\mathrm{p}}^2(\tan^2\alpha+2\lambda-\lambda^2)}}. \tag{11}$$

For the same axial piston pump, the ratio of speed limitation at two different inlet pressures (P_{in1} and P_{in2}) can be given as

$$\frac{\omega_{\max1}}{\omega_{\max2}}=\sqrt{\frac{P_{\mathrm{in1}}-p_{\mathrm{a}}}{P_{\mathrm{in2}}-p_{\mathrm{a}}}}, \tag{12}$$

where $\omega_{\max1}$ and $\omega_{\max2}$ are the speed limitations corresponding to P_{in1} and P_{in2}, respectively.

4 Scaling law for axial piston pumps

For convenience and economic feasibility, most manufacturers design a family of axial piston pumps by scaling a well-designed baseline product. For example, axial piston pumps used in aerospace applications are often characterized as having high rotational speed and small volumetric displacement. For practical importance, pump engineers design such high-speed and small-size aviation pumps on the basis of one successful commercial product that is widely used in construction machinery and has a relatively large unit size but low speed capacity. For experienced pump engineers, the first step to such design is to estimate the pump's speed limitation for a desired volumetric displacement. This critical speed estimation cannot be completed without considering the cavitation constraint governed by Eq. (11).

Equation (11) can be used to derive the relationship between the speed limitation of a new scaled machine and that of the baseline one, as follows:

$$\frac{\omega'_{\max}}{\omega_{\max}} = \frac{R_p}{R'_p}\left[\frac{\rho(\tan^2\alpha + 2\lambda - \lambda^2)(P'_{in} - p'_a)}{\rho'(\tan^2\alpha' + 2\lambda' - \lambda'^2)(P_{in} - p_a)}\right]^{1/2}, \quad (13)$$

where the unprimed and primed notations represent variables related to the baseline design and newly scaled design, respectively.

Volumetric displacement V_g is a function of the pump's geometric parameters.

$$V_g = 2N\pi r_p^2 R_p \tan\alpha, \quad (14)$$

where N denotes the piston number.

By substituting Eq. (14) into Eq. (13) to eliminate the variable R_p, we can establish the relationship between speed limitation and volumetric displacement as follows:

$$\frac{\omega'_{\max}}{\omega_{\max}} = \left(\frac{V_g}{V'_g}\right)^{1/3}\left(\frac{N'\lambda'^2\tan\alpha'}{N\lambda^2\tan\alpha}\right)^{1/3} \times \left[\frac{\rho(\tan^2\alpha + 2\lambda - \lambda^2)(P'_{in} - p'_a)}{\rho'(\tan^2\alpha' + 2\lambda' - \lambda'^2)(P_{in} - p_a)}\right]^{1/2}. \quad (15)$$

In practical cases, the swash plate angle, hydraulic oil, and inlet pressure often remain unchanged in both machines. Thus, Eq. (15) can be greatly simplified to

$$\frac{\omega'_{\max}}{\omega_{\max}} = \left(\frac{V_g}{V'_g}\right)^{1/3}\left(\frac{\lambda'}{\lambda}\right)^{2/3}\left(\frac{\tan^2\alpha + 2\lambda - \lambda^2}{\tan^2\alpha' + 2\lambda' - \lambda'^2}\right)^{1/2}. \quad (16)$$

Generally, the ratio λ of piston radius to the piston pitch radius remains relatively constant for a family of machines. Table 1 presents an example of the statistical results of this ratio for different unit sizes, in which the ratio λ is kept steady at about 0.25. Assuming that the ratio λ also remains the same between machines, Eq. (16) can be further simplified to produce a scaling law that can estimate the speed limitation of a new machine.

$$\frac{\omega'_{\max}}{\omega_{\max}} = \left(\frac{V_g}{V'_g}\right)^{1/3}. \quad (17)$$

Equation (17) indicates that the maximum rotational speed of a new machine is inversely proportional to its cube root of volumetric displacement. That is to say, a small volumetric displacement allows for a high speed limitation for axial piston machines.

5 Results and discussion

The scaling law in Eq. (17) aims to estimate the speed limitation at which the newly scaled axial piston machines are free from cavitation. Three strategies can be used to examine the validity of the scaling law. The first indirect strategy is to compare the estimated and experimental critical inlet pressures of an axial piston pump, where the estimated value is obtained with Eq. (10). Another indirect strategy involves verifying the relationship between the required inlet pressure and speed limitation, as shown in Eq. (12). The third strategy is to validate the scaling law directly by using the information on volumetric displacement and speed limitation available in open product brochures.

Table 1 Comparison of ratio λ for a family of axial piston pumps

Volumetric displacement, V_g/(mL·r^{-1})	Piston radius, r_p/mm	Piston pitch radius, R_p/mm	Ratio, λ
28	7.50	32.2	0.23
45	9.00	34.5	0.26
80	10.00	39.5	0.25
125	12.25	51.0	0.24

A closed-loop hydraulic system was built in this study to determine the critical inlet pressure of a high-speed axial piston pump experimentally, as shown in Fig. 3. A detailed description of the hydraulic system is presented in Ref. [20]. The tested pump was operated at a constant rotational speed of 10000 r/min and discharge pressure of 16 MPa. The inlet pressure of the pump could be regulated, and it was initially set to be high enough to avoid cavitation. When the working conditions of the tested pump reached the steady state, the relative pressure of the inlet port was adjusted from 0.3 to 0 MPa, and the flow rates of the drain and outlet ports were recorded simultaneously.

Figure 4 shows the influence of inlet pressure on the delivery flow rate, which considers the leakage flow rate. The full delivery flow rate at high inlet pressures revealed the absence of cavitation in the pump. However, when the inlet pressure dropped to below 0.10 MPa, cavitation occurred, and the delivery flow rate decreased sharply. The estimated and actual critical inlet pressures are also compared in Fig. 4, in which the actual critical inlet pressure is approximately 0.10 MPa and the estimated one calculated by Eq. (10) is 0.03 MPa. The close values of the estimated and actual critical inlet pressures give us confidence in the analytical cavitation model. The estimated value was lower than the actual value possibly because for mathematical simplicity, Eq. (10) does not consider the pressure head to overcome the flow resistance along the suction line and the local loss caused by flow passage contraction and enlargement.

The cavitation model can be also examined with Eq. (12), which describes the variation of the maximum allowable rotational speed as the inlet pressure. A comparison of the estimated and actual speed limitations is presented in Tables 2–4, where all the actual data presented are available in the open product brochures from each pump manufacturer. Table 2 compares the ratios of

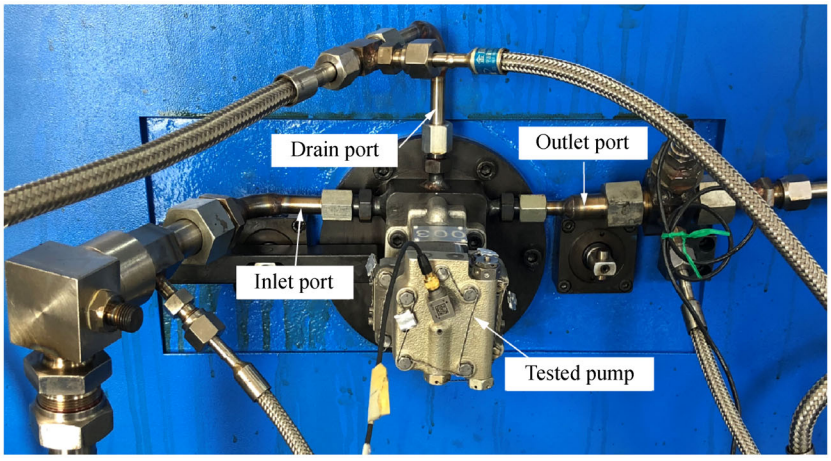

Fig. 3 Tested high-speed axial piston pump.

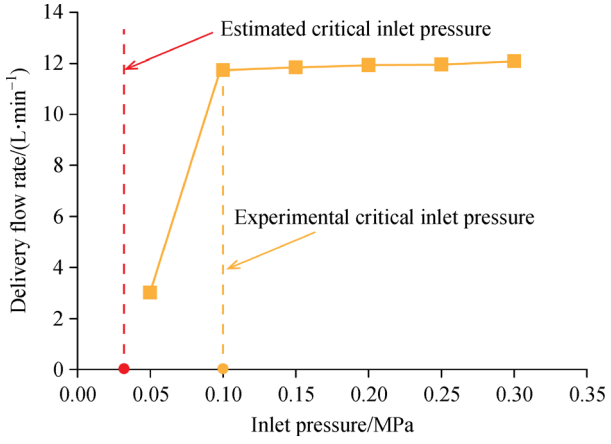

Fig. 4 Experimental delivery flow rates at various inlet pressures.

the maximum rotational speeds, $\omega_{max1}/\omega_{max2}$, at relative inlet pressures of 0.15 and 0.10 MPa for different unit sizes of Parker F11 pumps. The estimated value of $\omega_{max1}/\omega_{max2}$ for each unit size was calculated using Eq. (12). The calculation error of $\omega_{max1}/\omega_{max2}$ in Table 2 ranges only between –0.52% and 3.53%, which indicates good agreement between the estimated and actual speed limitations.

Tables 3 and 4 present the comparison results of speed limitation for Rexroth A4VSO and A10VSO open-circuit pumps. Unlike the product brochures of Parker pumps, those of Rexroth pumps provide data on $\omega_{max1}/\omega_{max2}$ instead of specific speed limitations. In Tables 3 and 4, ω_{max2} is the reference speed limitation at an absolute inlet pressure of 0.10 MPa, and ω_{max1} is the speed limitation at another absolute inlet pressure, such as 0.08, 0.09, 0.10, 0.12, 0.14, and 0.16 MPa. Tables 3 and 4 indicate that most of the calculation errors are less than 15% and acceptable for the preliminary design of a new pump in engineering applications. A possible explanation for the overestimated speed limitation at high inlet pressures is that Eq. (12) does not consider other restriction factors, such as the tilting motion of the rotating group and the pressure–velocity value of lubricating interfaces. In other words, the two physical factors mentioned above restrain the increment in speed limitation with increasing inlet pressures according to Eq. (12).

To further examine the scaling law in industrial practice, we plotted the estimated and actual speed limitations versus the volumetric displacements for axial piston machines from three popular manufacturers. The speed limitation results of Vickers, Parker, and Rexroth pumps are shown in Figs. 5–7, respectively. All of the actual data in these figures were obtained from the open product brochures of each pump manufacturer. The solid line in each figure represents the speed limitation

Table 2 Speed limitation estimation for Parker F11 pumps

Volumetric displacement, V_g/(mL·r^{-1})	Relative inlet pressure, P_{in1}/MPa	Relative inlet pressure, P_{in2}/MPa	Speed limitation, ω_{max1}/(r·min^{-1})	Speed limitation, ω_{max2}/(r·min^{-1})	Actual $\omega_{max1}/\omega_{max2}$	Calculated $\omega_{max1}/\omega_{max2}$	Calculation error/%
4.9	0.15	0.10	8400	7300	1.151	1.145	–0.52
9.8	0.15	0.10	7300	6400	1.141	1.145	0.35
12.5	0.15	0.10	6300	5600	1.125	1.145	1.78
14.3	0.15	0.10	6300	5600	1.125	1.145	1.78
19.0	0.15	0.10	5200	4700	1.106	1.145	3.53

Table 3 Speed limitation estimation for Rexroth A4VSO pumps

Absolute inlet pressure, P_{in1}/MPa	Actual $\omega_{max1}/\omega_{max2}$	Calculated $\omega_{max1}/\omega_{max2}$	Calculation error/%
0.08	0.89	0.82	7.9
0.10	–	–	–
0.12	1.06	1.15	8.5
0.14	1.14	1.29	13.2
0.16	1.18	1.41	19.5

Table 4 Speed limitation estimation for Rexroth A10VSO pumps

Absolute inlet pressure, P_{in1}/MPa	Actual $\omega_{max1}/\omega_{max2}$	Calculated $\omega_{max1}/\omega_{max2}$	Calculation error/%
0.08	0.90	0.82	9.8
0.09	0.95	0.91	4.2
0.10	–	–	–
0.12	1.07	1.15	7.5
0.14	1.12	1.29	15.2
0.16	1.17	1.41	20.5

recommendation derived from Eq. (17), and the scatter data represent the actual speed limitation recommended by the pump manufacturers. The plots in Figs. 5–7 indicate that Eq. (17) addressed the basic scaling issue with small acceptable deviations. The average prediction accuracies of speed limitation for Vickers PV, Parker F12, and Rexroth A10VSO and A11VO pumps were 91.2%, 96.4%, 98.8%, and 95.0%, respectively. Therefore, with reasonable confidence, Eq. (17) can be regarded as the general scaling law for the speed limitation of axial piston machines.

A practical characteristic constant C_p of axial piston pumps can be derived by rearranging Eq. (17) as follows:

$$C_p = \omega_{max} V_g^{1/3} = \omega'_{max} (V'_g)^{1/3}, \tag{18}$$

where the characteristic constant has a velocity dimension

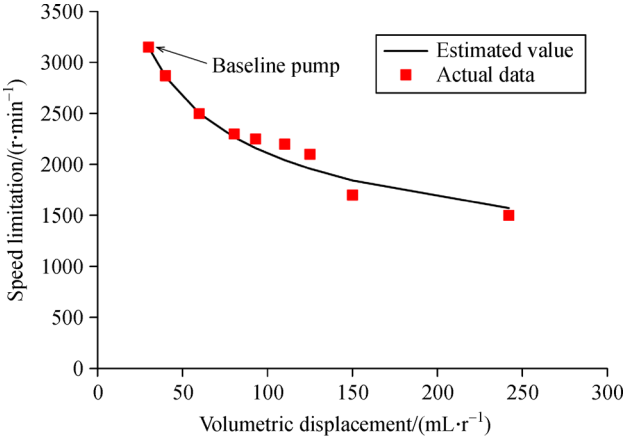

Fig. 6 Speed limitation estimation for Parker F12 pumps.

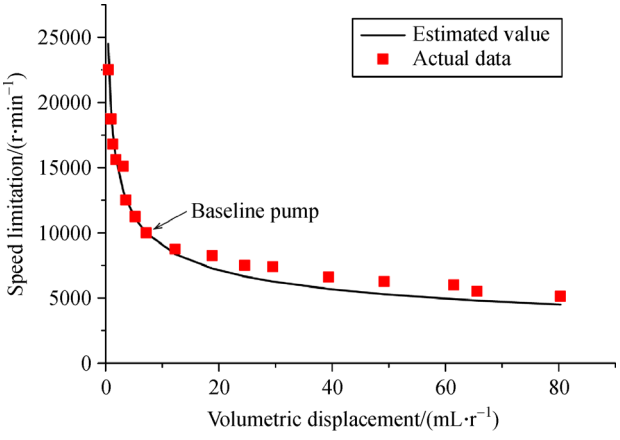

Fig. 5 Speed limitation estimation for Vickers PV pumps applied in aerospace applications.

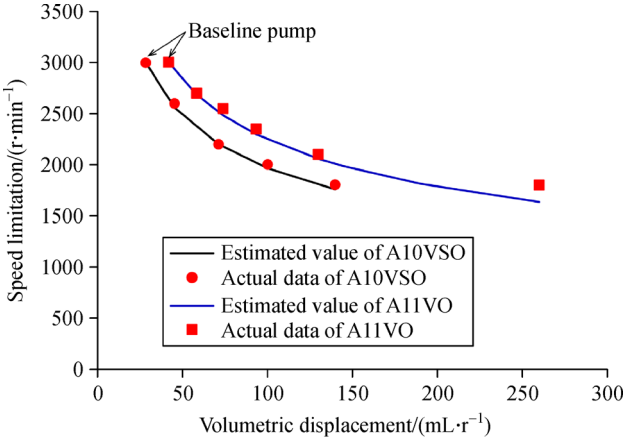

Fig. 7 Speed limitation estimation for Rexroth A10VSO and A11VO pumps.

and can thus represent the maximum flow velocity of the fluid flow in the rotating cylinder block. An excessively high flow velocity leads to cavitation according to the Bernoulli equation.

Figure 8 summarizes the values of C_p from several popular pump manufacturers, including Rexroth, Linde, Vickers, Parker, and Kawasaki. Figure 8 indicates that the C_p levels remain relatively stable for the same series of machines. For example, the C_p levels of Parker F12 and Rexroth A10VSO are maintained at about 9880 and 9220 $(r\cdot min^{-1})\cdot(mL\cdot r^{-1})^{1/3}$, respectively. Meanwhile, the C_p levels are varied from one pump manufacturer to another even for different pump series from the same manufacturer. For example, the C_p levels of Vickers PV pumps are much higher than those of other pumps mainly because Vickers PV pumps are used in aerospace applications, and their speed capacity is usually greatly improved by boosting the inlet pressure through the use of a pressurized reservoir or an integrated impeller. A10VSO and A11VO are open-circuit axial piston pumps, but the C_p levels of A11VO pumps are much higher than those of A10VSO pumps. This difference can be explained by the fact that A11VO pumps have spherical valve plates and inclined cylinder bores, whereas A10VSO pumps are equipped with flat valve plates and parallel cylinder bores. A spherical valve plate design reduces the pitch diameter of cylinder ports, and a low circumferential velocity equates to a small pressure loss of the entering flow. Moreover, the specially designed inclined cylinder bores further improve the suction performance of A11VO pumps due to the centrifugal effects of the rotating fluid. Notably, the speed capacity of the closed-circuit pumps (A4VSG and Linde HPV-02) in this study was much higher than that of the open-circuit pumps (A4VSG and Linde HPV-02). This result could be due to the integrated charge pump used for the closed-circuit pumps that helps improve suction performance.

6 Conclusions

The following conclusions were obtained from the analysis, results, and discussion in this study.

1) The cavitation phenomenon in the displacement chambers is a critical factor that restricts the speed limitation of axial piston pumps. The pressure loss contributing to the cavitation mainly results from the entering flow's accelerated movement along the cylinder bores and the rotating movement together with the cylinder block.

2) The minimum required inlet pressure and the speed limitation of axial piston pumps can be derived based on the analytical model of cavitation, as shown in Eqs. (10) and (11). For a given axial piston machine, its speed limitation can benefit from increasing the inlet pressure, as shown in Eq. (12), where the speed limitation is approximately proportional to the square root of the inlet pressure.

3) The scaling law in Eq. (17) describes the relationship between speed limitation and volumetric displacement; that is, the speed limitation of a newly scaled axial piston machine is inversely proportional to the cube root of volumetric displacement. In other words, a small volumetric displacement or unit size equates to a high speed capacity for axial piston machines. This useful scaling law was verified in this study by using actual specification data from open product brochures.

4) Derived from the scaling law, the characteristic constant C_p (Eq. (18)) describes a comprehensive constraint of cavitation on speed limitation and volumetric displacement. This practical parameter represents the permissible maximum velocity of the entering flow to

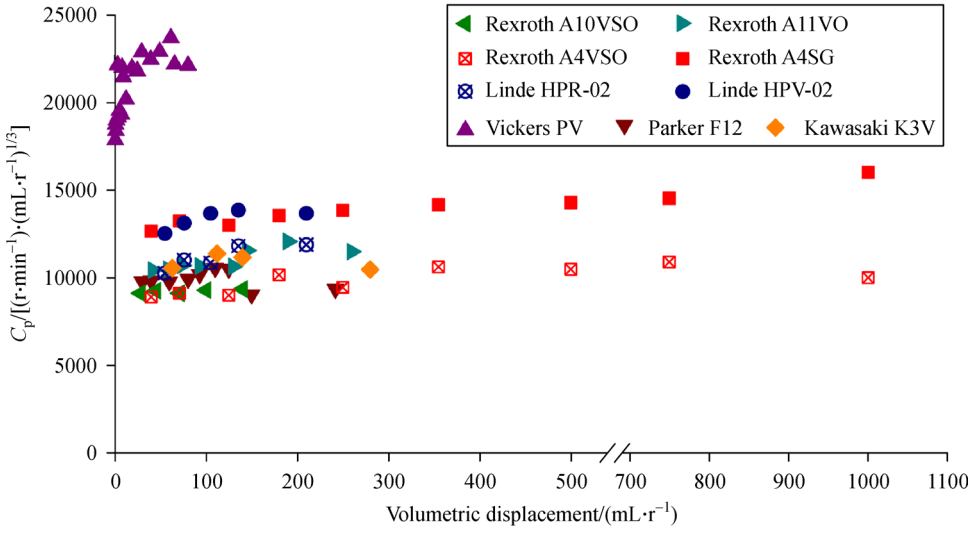

Fig. 8 C_p values for axial piston pumps produced by different manufacturers.

avoid cavitation in the displacement chambers. The statistical data collected from several pump manufacturers showed that the C_p level is about 9000–13000 $(r\cdot min^{-1})\cdot(mL\cdot r^{-1})^{1/3}$ for general industrial applications and 18000–23000 $(r\cdot min^{-1})\cdot(mL\cdot r^{-1})^{1/3}$ for aerospace applications. Engineering measures for improving the C_p level include the use of a pressurized reservoir, boosting impeller, spherical valve plate, and cylinder block with inclined bores.

Acknowledgements This work was supported by the China National Postdoctoral Program for Innovative Talents (Grant No. BX20200210), the China Postdoctoral Science Foundation (Grant No. 2019M660086), and the Common Technology for Equipment Pre-research Project (Grant No. 41402050202).

References

1. Tanaka Y, Sakama S, Nakano K, et al. Comparative study on dynamic characteristics of hydraulic, pneumatic and electric motors. In: Proceedings of ASME/BATH 2013 Symposium on Fluid Power and Motion Control. Sarasota: ASME, 2013, V001T01A037
2. Manring N D, Mehta V S, Nelson B E, et al. Increasing the power density for axial-piston swash-plate type hydrostatic machines. Journal of Mechanical Design, 2013, 135(7): 071002
3. Kunkis M, Weber J. Experimental and numerical assessment of an axial piston pump's speed limit. In: Proceedings of BATH/ASME 2016 Symposium on Fluid Power and Motion Control. Bath: ASME, 2016, V001T01A048
4. Wu S, Yu B, Jiao Z, et al. Preliminary design and multi-objective optimization of electro-hydrostatic actuator. Proceedings of the Institution of Mechanical Engineers, Part G: Journal of Aerospace Engineering, 2017, 231(7): 1258–1268
5. Alle N, Hiremath S S, Makaram S, et al. Review on electro hydrostatic actuator for flight control. International Journal of Fluid Power, 2016, 17(2): 125–145
6. Chao Q, Zhang J, Xu B, et al. A review of high-speed electro-hydrostatic actuator pumps in aerospace applications: Challenges and solutions. Journal of Mechanical Design, 2019, 141(5): 050801
7. Harris R M, Edge K A, Tilley D G. Predicting the behavior of slipper pads in swashplate-type axial piston pumps. Journal of Dynamic Systems, Measurement, and Control, 1996, 118(1): 41–47
8. Manring N D. Slipper tipping within an axial-piston swash-plate type hydrostatic pump. In: Proceedings of ASME International Mechanical Engineering Congress and Exposition. Anaheim: ASME, 1998, 169–175
9. Borghi M, Specchia E, Zardin B, et al. The critical speed of slipper bearings in axial piston swash plate type pumps and motors. In: Proceedings of ASME 2009 Dynamic Systems and Control Conference. Hollywood: ASME, 2009, 267–274
10. Manring N D. Tipping the cylinder block of an axial-piston swash-plate type hydrostatic machine. Journal of Dynamic Systems, Measurement, and Control, 2000, 122(1): 216–221
11. Achten P, Eggenkamp S. Barrel tipping in axial piston pumps and motors. In: Proceedings of the 15th Scandinavian International Conference on Fluid Power. Linköping, 2017, 381–391
12. Zhang J, Chao Q, Xu B. Analysis of the cylinder block tilting inertia moment and its effect on the performance of high-speed electro-hydrostatic actuator pumps of aircraft. Chinese Journal of Aeronautics, 2018, 31(1): 169–177
13. Halat J A. Hydraulic Pumps for High Pressure Non-Flammable Fluids. SAE Technical Paper 2000-01-2581, 1985
14. Chao Q, Zhang J, Xu B, et al. Centrifugal effects on cavitation in the cylinder chambers for high-speed axial piston pumps. Meccanica, 2019, 54(6): 815–829
15. Chao Q, Zhang J, Xu B, et al. Effects of inclined cylinder ports on gaseous cavitation of high-speed electro-hydrostatic actuator pumps: A numerical study. Engineering Applications of Computational Fluid Mechanics, 2019, 13(1): 245–253
16. Wang Y, Dong H, He Y. A novel approach for predicting inlet pressure of aircraft hydraulic pumps under transient conditions. Chinese Journal of Aeronautics, 2019, 32(11): 2566–2576
17. Dong H, Wang Y, Chen J. First attempt to determine the critical inlet pressure for aircraft pumps with a numerical approach that considers vapor cavitation and air aeration. Proceedings of the Institution of Mechanical Engineers, Part G: Journal of Aerospace Engineering, 2020, 234(12): 1926–1938
18. Vacca A, Klop R, Ivantysynova M. A numerical approach for the evaluation of the effects of air release and vapour cavitation on effective flow rate of axial piston machines. International Journal of Fluid Power, 2010, 11(1): 33–45
19. Gullapalli S, Michael P, Kensler J, et al. An investigation of hydraulic fluid composition and aeration in an axial piston pump. In: Proceedings of ASME/BATH 2017 Symposium on Fluid Power and Motion Control. Sarasota: ASME, 2017, V001T01A028
20. Chao Q, Tao J, Wei X, et al. Identification of cavitation intensity for high-speed aviation hydraulic pumps using 2D convolutional neural networks with an input of RGB-based vibration data. Measurement Science and Technology, 2020, 31(10): 105102
21. Fey C G, Totten G E, Bishop R J, et al. Analysis of Common Failure Modes of Axial Piston Pumps. SAE Technical Paper 2000-01-2581, 2000
22. Frosina E, Marinaro G, Senatore A. Experimental and numerical analysis of an axial piston pump: A comparison between lumped parameter and 3D CFD approaches. In: Proceedings of ASME-JSME-KSME 2019 the 8th Joint Fluids Engineering Conference. San Francisco: ASME, 2019, V001T01A042
23. Schleihs C, Viennet E, Deeken M, et al. 3D-CFD simulation of an axial piston displacement unit. In: Proceedings of the 9th International Fluid Power Conference. Aachen, 2014, 332–343
24. Li T. Study on bootstrap reservoir type pressurized system for civil aircraft hydraulic supply system. In: Proceedings of 2016 IEEE International Conference on Aircraft Utility Systems (AUS). Beijing: IEEE, 2016, 1117–1121
25. Eaton. Engine-driven pump model PV3-240-18. Available at Eaton website, 2020-7-30
26. Mohn G, Nafz T. Swash plate pumps—The key to the future. In: Proceedings of the 10th International Fluid Power Conference. Dresden: Dresden University of Technology, 2016, 139–150
27. Bügener N, Helduser S. Analysis of the suction performance of axial

piston pumps by means of computational fluid dynamics (CFD). In: Proceedings of the 7th International Fluid Power Conference. Aachen, 2010

28. Bügener N, Klecker J, Weber J. Analysis and improvement of the suction performance of axial piston pumps in swash plate design. International Journal of Fluid Power, 2014, 15(3): 153–167
29. Kosodo H. Development of micro pump and micro-HST for hydraulics. JFPS International Journal of Fluid Power System, 2012, 5(1): 6–10
30. Wang S. The analysis of cavitation problems in the axial piston pump. Journal of Fluids Engineering, 2010, 132(7): 074502
31. Shi Y, Lin T, Meng G, et al. A study on the suppression of cavitation flow inside an axial piston pump. In: Proceedings of 2016 Prognostics and System Health Management Conference. Chengdu: IEEE, 2016
32. Manring N D, Mehta V S, Nelson B E, et al. Scaling the speed limitations for axial-piston swash-plate type hydrostatic machines. Journal of Dynamic Systems, Measurement, and Control, 2014, 136(3): 031004
33. Svedberg G C, Totten G E, Sun Y H, et al. Hydraulic system cavitation: Part II—A review of hardware design-related effects. SAE Transactions, 1999, 108: 385–397
34. Bishop R J, Totten G E. Effect of pump inlet conditions on hydraulic pump cavitation: A review. In: Totten G, Wills D, Feldmann D, eds. Hydraulic Failure Analysis, Fluids, Components and System Effects. West Conshohocken: ASTM International, 2001, 318–332
35. Hibi A, Ibuki T, Ichikawa T, et al. Suction performance of axial piston pump: 1st report, analysis and fundamental experiments. Bulletin of the JSME, 1977, 20(139): 79–84